

Large p_T Hadroproduction of Z as a Probe of Gluon Distribution inside Proton

C. S. Kim ^{*} and Jake Lee [†]

*Department of Physics, Yonsei University,
Seoul 120-749, Republic of Korea*

Abstract

The transverse momentum distribution of single vector boson production at hadron colliders provides useful ways of testing the Standard Model and searching new physics beyond the Standard Model. We study large p_T hadroproduction of Z -boson as a probe of gluon distributions inside proton. We investigate how to get initial gluon-involving contributions, or how to subtract quark-quark (or -antiquark) contributions from total cross section. We also investigated the simultaneous measurement of the rapidity and the transverse momentum of the produced Z boson, to obtain momentum fractions of initial partons. And we extracted relevant uncertainties involving in experimental and theoretical analyses. This large p_T hadroproduction of Z can be used as constraints on analyses of global parton (gluon and quarks) distribution functions inside proton.

^{*}e-mail : kim@cskim.yonsei.ac.kr

[†]e-mail : jilee@theory.yonsei.ac.kr

1 Introduction

The transverse momentum distribution of single vector boson production provides useful methods of testing the Standard Model and searching new physics beyond the Standard Model. Here we would like to investigate mainly the gluon distribution inside proton using large p_T production of Z -boson at hadron colliders.

The recent improvements in the data of deep-inelastic lepton-nucleus scattering and of the Drell-Yan process have allowed a definitive determination of the quark distribution functions inside the nucleon. However, the gluon distribution $G(x, Q^2)$ is not well constrained by these processes, since it only enters as a second-order effect. On the other hand, the gluon contributes to the lowest order for vector boson hadroproduction with large transverse momentum and it has become normal practice to use fixed-target $pp(\bar{p}) \rightarrow VX$ data to determine the gluon distribution for $x \sim 2p_T/\sqrt{s}$ (where V represents a vector boson and p_T is the transverse momentum of the produced vector boson). The prompt photon production $p\bar{p} \rightarrow \gamma X$ has been already used on that purpose [1, 2]. In principle, collider data obtained for $p\bar{p} \rightarrow \gamma X$ at the Fermilab energy ($\sqrt{s} = 1.8$ TeV) with $p_T \sim 10$ GeV could probe the gluon at $x \sim 10^{-2}$. However, a detailed study of uncertainties in the theoretical predictions of prompt-photon production at collider energies has shown that such determination will be difficult for some reasons [3, 4]. One problem is the importance of the bremsstrahlung component at small p_T , in which the photon is radiated from an outgoing quark and so occurs in the debris of a hadronic jet. A second ambiguity is related to the choice of scales in the parton distribution functions and the QCD coupling strength α_s . For these uncertainties, massive vector boson W or Z hadroproduction is more useful than γ . The bremsstrahlung W , Z processes are almost negligible; that is the outgoing quark (or anti-quark) will very rarely fragment into W or Z . And the choice of scales can be fixed more acceptably, for instance, as $Q^2 = M_W^2$ or M_Z^2 .

Previously, as an example, it was pointed out that W^\pm production could be used as measures for gluon and heavy quark distributions [4], which concentrated on the following subprocesses;

$$(i) \quad sg \rightarrow cW$$

$$(ii) \quad cg \rightarrow cZ.$$

They proposed (i) as a measure of the gluon, and the ratio of (ii) to (i) to determine the ratio c/s of quark densities. However, a W -boson possibly decays leptonically into $e\nu$. And because one cannot detect neutrinos, one could confirm W production only through detecting an electron and large missing p_T , which usually results in large systematic uncertainties. On the other hand, a Z -boson decays leptonically to e^+e^- , so we can confirm Z production with less systematic uncertainties. Pacing with considerable new data of Z hadroproduction at Tevatron, we would like to investigate gluon densities of proton by using large p_T hadroproduction of Z . At a glance, it seems possible to use the above subprocess, (ii) $cg \rightarrow cZ$, as a probe of gluon. But it is not so effective, since this subprocess involves the initial charm quark, and the resulting cross section would be very small. As one can see more details later, we instead use initial qg subprocesses, where q represents any of three light quarks.

In this letter, we present the transverse momentum and rapidity distributions of Z boson, calculated up to the second order in QCD coupling. When the produced Z has small transverse momentum p_T , there are large logarithms $\log(Q^2/p_T^2)$, and perturbation theory for $d\sigma/dp_T^2$ breaks down there. And one must either perform a resummation or restrict attention to the total cross section by integrating analytically in p_T . These techniques have been carried out to the first order in QCD [5], and part of the second-order terms have been analyzed in the $p_T \rightarrow 0$ limit [6]. Therefore, we here restrict ourselves to the region of large p_T to avoid these difficulties in small p_T . In the references [7, 8], the full analytic formulae of $d\sigma/dp_T^2 dy$ for

large p_T vector boson production up to the second order in QCD had been already presented. Based on those formulae we study the gluon distribution inside proton through large p_T hadroproduction of Z -boson. By including the full $\alpha\alpha_s^2$ contributions, we are able to considerably reduce the theoretical errors, normally associated with the leading order ($O(\alpha\alpha_s)$) results. We calculated $K \equiv d\sigma_2(Z)/d\sigma_1(Z)$ as a function of $p_T(Z)$, where $d\sigma_n$ denotes the differential cross section $d\sigma/dp_T(Z)$ including all QCD subprocesses up to $O(\alpha\alpha_s^n)$ at $\sqrt{s} = 1.8$ TeV using $Q^2 = M_Z^2$, and found that $K \simeq 1.3 \sim 1.4$ for $p_T(Z) \geq 10\text{GeV}$. The corrections are significant, but show that the perturbative expansion is reasonable.

Up to the order of $\alpha\alpha_s^2$, $p\bar{p} \rightarrow ZX$ process includes initial $q\bar{q}$ (qq or $\bar{q}\bar{q}$), qg ($\bar{q}g$) and gg scatterings in partonic level. Among these subprocesses, only qg ($\bar{q}g$) and gg scatterings are initial gluon-involving parts. Therefore, one can analyze the gluon distribution by subtracting initial quark-quark contributions from the total subprocesses of Z hadroproduction. At the Tevatron energies the contribution from initial gg part is very small, and we can ignore in the numerical analyses.

2 Detailed investigations of gluon distribution

As mentioned in Section 1, we would like to use the formulae of reference [7] for our detailed analyses. The authors of [7] presented the hadronic cross sections up to the order of $\alpha\alpha_s^2$ for $A + B \rightarrow \gamma^* + jet(s)$,

$$\frac{d\sigma_{AB}}{dp_T^2 dy} = \sum_{i,j} \int dx_1 dx_2 f_i^A(x_1, Q^2) f_j^B(x_2, Q^2) \frac{sd\tilde{\sigma}}{dt du}(\alpha_s(Q^2), x_1 P_1, x_2 P_2) ,$$

where A and B are the initial hadrons, P_i are their momenta, and $d\tilde{\sigma}$ is the factorized partonic cross section in the \overline{MS} factorization scheme.

The large p_T hadroproduction of Z up to $\alpha\alpha_s^2$ can be calculated by the characteristic five groups of diagrams, as follows

$$(i) \quad q\bar{q} \rightarrow gZ,$$

- (ii) Next-to-leading diagrams for $q\bar{q} \rightarrow gZ$,
- (iii) $q\bar{q} \rightarrow ggZ$,
- (iv) $q\bar{q} \rightarrow q\bar{q}Z$,
- (v) $qq \rightarrow qqZ$.

Diagrams (i) are the first-order ones for Z production through $q\bar{q}$ annihilation. Parts of the second-order contribution come from the interference of these diagrams with the one-loop corrections of diagrams (ii). The rest comes from 2-*jet* productions accompanying the Z , such as the diagrams (iii). The diagrams through initial qg -scattering can be obtained from (i), (ii) and (iii) by crossing them. The diagrams through gg -scattering can be similarly obtained from (iii) alone. The diagrams (iv) give the remaining parts to $q\bar{q}$ -scattering. And the diagrams (v) are for qq -scattering for Z hadroproduction. Therefore, we have three types of contributions for Z hadroproduction

- $QQ \rightarrow Z + 1 \text{ or } 2jets$,
- $QG \rightarrow Z + 1 \text{ or } 2jets$,
- $GG \rightarrow Z + 2jets$,

where Q represents initial parton of a quark or anti-quark, and G for a gluon.

To further investigate our observations, we numerically calculate the transverse momentum p_T , and the rapidity y distributions of Z at the Tevatron energies including all QCD subprocesses up to the order α_s^2 in $p\bar{p}$ collisions. We use three input parton distribution functions; MRS(A) [9], GRV(HO) [10] and CTEQ3 [11]. Fig. 1 shows p_T distributions using three parton distributions at $\sqrt{s} = 1.8$ TeV, where we use $Q^2 = M_Z^2$, and include three light quarks (u, d, s) as initial quark-partons. As mentioned earlier, initial GG -scattering part is very small, and we do not show it explicitly here. (Of cause, we include GG -part to calculate total cross section.) We find that their gluon distributions are almost same at $Q^2 \sim M_Z^2$, and

in Fig. 1 the deviations of distributions are mainly due to the difference of sea-quark distributions. We also note from Fig. 1 that it looks very important to subtract the initial QQ -contributions to extract contributions involving gluons only. However, the $p\bar{p} \rightarrow Z + jets$ process contains many different subprocesses, and it might be impossible to distinguish the initial QQ -contributions from the QG -ones *experimentally* by analyzing shapes of final hadronic jets, and *etc.* Now that we have theoretical predictions of the initial QQ -contributions, we can in principle subtract those from the experimental total result. And by comparing the remaining experimental cross section and theoretical one, one can probe the gluon distributions inside proton. However, as can be seen in Fig. 1 for $p_T \geq 10$ GeV, QQ -contributions are about 70% of total cross section, and it looks inappropriate to subtract QQ -part, which is not a minor part, but a major contribution. Therefore, one should raise p_T minimum cut up to about $40 \sim 50$ GeV, to make QQ - and QG -contributions at least experimentally comparable. These practical considerations will be presented in more detail in Section 3.

Assuming that we could experimentally distinguish $Z + 1jet$ from $Z + 2jets$, let us first consider simple $Z + 1jet$ case. In partonic level, $p\bar{p} \rightarrow Z + 1jet$ process includes only two types of diagrams;

- $q\bar{q} \rightarrow Zg$,
- $qg \rightarrow Zq$ (or $\bar{q}g \rightarrow Z\bar{q}$).

In these processes, we can extract initial gluon-involving contributions by subtracting *theoretical* prediction of $q\bar{q} \rightarrow Zg$ subprocess from the *experimental* total results of $p\bar{p} \rightarrow Z + 1jet$. Furthermore, if we could distinguish the *quark-jet* from the *gluon-jet* through theoretical and experimental combined analyses, only the initial gluon contributing part can be extracted experimentally from $Z + 1 quark-jet$. Fig. 2 shows the p_T distributions of $Z + 1jet$ from $q\bar{q} \rightarrow Zg$ and $qg \rightarrow Zq$ ($\bar{q}g \rightarrow Z\bar{q}$). For comparison, we also show p_T distributions of $p\bar{p} \rightarrow Z + 1jet$ and $Z + 2jets$.

Until now we have only considered the transverse momentum p_T distributions. We now consider analyses with simultaneous measurement of both rapidity y and p_T of the produced Z boson. The y and p_T of the Z boson in the laboratory frame are related to the momentum fractions of initial partons by

$$\begin{aligned} y &= \frac{1}{2} \ln \frac{E + p_L}{E - p_L} \\ &= \ln \left\{ \frac{M_Z^2 + x_1 x_2 s - s_2}{2x_2 \sqrt{s} (M_Z^2 + p_T^2)^{1/2}} \pm \sqrt{\frac{(M_Z^2 + x_1 x_2 s - s_2)^2}{(2x_2 \sqrt{s} (M_Z^2 + p_T^2)^{1/2})^2} - \frac{x_1}{x_2}} \right\}, \end{aligned} \quad (1)$$

where s is the invariant mass of the incoming hadrons, and s_2 is the invariant mass of final two-jets *when two jets accompany the produced Z* . And x_1, x_2 are the four-momentum fractions of the colliding partons. If we consider only $Z + 1jet$ processes, the value of s_2 in the above relation becomes zero. By using the above relation we can directly obtain the gluon momentum fraction inside incoming proton.

3 Discussions

We now study relevant uncertainties in analyzing large p_T hadroproduction of Z , which one must take into account in theoretical and experimental analyses. The first uncertainty comes from QCD-scale dependences. Although there is much less ambiguity associated with the choice of scales compared to direct photon case, as explained before, there still remains weak QCD-scale dependence because of considering only finite order of perturbative corrections. In Table 1 we give total cross sections for $p\bar{p} \rightarrow ZX$ production integrated over the region $p_T(Z) > p_{min}^Z = 10$ GeV for various Q^2 . The value of p_{min}^Z is chosen so as to retain as many clear events as possible and yet to remain in a region where perturbation theory gives a reliable prediction. The same scale is chosen for the parton densities and QCD strength $\alpha_s(Q^2)$. But these scales need not be the same. Table 2 shows the sensitivity, when we choose different scales for $\alpha_s(Q^2)$ and parton distribution functions. We note that there show significant differences in results between $Q^2 = M_Z^2$ and $Q^2 = p_T^2/2$

Table 1: *The integrated total cross sections with the same scales for α_s and parton distributions.*

$\sigma (nb)$	$p_T > 10 GeV, \quad y < 2.5$			
scale Q^2	M_Z^2	$p_T^2/2$	p_T^2	$2p_T^2$
MRS(A)	1.84	2.16	2.06	1.99
GRV(HO)	1.73	2.05	1.95	1.88
CTEQ3	1.87	2.19	2.10	2.02

for parton distributions, where we fix the scale of $\alpha_s(Q^2)$ as M_Z^2 , as in Table 2. Therefore, once we have sufficient experimental data for this process ($p\bar{p} \rightarrow ZX$), we could even investigate scale dependence of QCD-coupling α_s , as well as parton distribution functions.

Table 2: *The integrated total cross sections with different scales for α_s and parton distributions. We fix $Q^2 = M_Z^2$ for α_s and use four different scales for parton distribution functions.*

$\sigma (nb)$	$p_T > 10 GeV, \quad y < 2.5$			
scale Q^2	M_Z^2	$p_T^2/2$	p_T^2	$2p_T^2$
MRS(A)	1.84	1.52	1.59	1.64
GRV(HO)	1.73	1.43	1.50	1.54
CTEQ3	1.87	1.54	1.61	1.66

Next we still have uncertainties related to structure functions of initial quarks, when we try to derive informations on gluon. Here we use three different parametrizations; MRS(A), GRV(HO), CTEQ3. Martin *et. al.* [9] improved their parametrization of parton densities through a new global analysis on deep inelastic scatterings and related data including the recent measurements of F_2 at HERA, on the asymmetry of the rapidity distributions of W^\pm production [12] at Tevatron, and on the asymmetry in Drell-Yan production in pp and pn collisions [13]. We use their latest version of MRS(A) functions. CTEQ Collaboration [11] also improved their distribution functions, incorporating several new types of data and presented the new

version CTEQ3, which we use here. Glück *et. al.* [10] predicted the parton distributions down to $x \simeq 10^{-4}$ and $Q^2 \simeq 0.3 \text{ GeV}^2$, using the data from deep inelastic scattering experiments at $x \geq 10^{-2}$ together with the idea that at some low resolution scale the nucleon consists entirely of valence quarks and *valence*-like gluons. They presented parton distributions obtained for the leading order (GRVLO) as well as for the higher order (GRVHO) calculation. We use GRVHO.

The simultaneous measurement of y and p_T would enable us to determine the momentum fractions of initial partons from Eq. (1), and it was previously pointed out that one should be very careful in dealing with s_2 , where s_2 is the invariant mass of final state two jets,

$$s_2 = (p_{jet1} + p_{jet2})^2.$$

If only one jet presents in the final states, $s_2 = 0$ in our massless parton level approximation, as explained before. Experimenalists should find here the best optimized solution through realistic Monte Carlo studies to differentiate one-jet from two-jets final states, which are accompanying the produced Z -boson. Fig. 3 shows the p_T distributions of $p\bar{p} \rightarrow Z + jets$ for $y = 0$.

We next calculate numerically the number of events at Tevatron energies. For $|y| < 2.5$ and $p_T \geq 10 \text{ GeV}$, we get

$$\begin{aligned} \text{Number of events}/10pb^{-1} &= [2.00 \pm 0.15] \times 10^4 \quad \text{for MRS(A),} \\ &= [1.89 \pm 0.16] \times 10^4 \quad \text{for GRV(HO),} \\ &= [2.03 \pm 0.16] \times 10^4 \quad \text{for CTEQ3,} \end{aligned}$$

where the errors are such that the lower and upper limits correspond to the scale choice of $Q^2 = M_Z^2$ and $Q^2 = p_T^2/2$, respectively. As previously mentioned, about 70% of the above events is from the initial QQ -contributions, and QG -contributions, which we are interested in for our investigation of gluon distributions, are only 30% of total events. It would not be so effective to subtract from total number of events

QQ -contributions, which are much larger than QG -ones. Therefore, we need raise p_T minimum cut to make initial QG -contributions at least comparable to QQ -ones. Fig. 4 shows the rapidity distributions with (a) $p_T \geq 10$ GeV, and (b) $p_T \geq 40$ GeV. And for $|y| < 2.5$ and $p_T \geq 40$ GeV, we get

$$\begin{aligned}
\text{Number of events}/10pb^{-1} &= [2.27 \pm 0.07] \times 10^3 \quad \text{for MRS(A),} \\
&= [2.18 \pm 0.07] \times 10^3 \quad \text{for GRV(HO),} \\
&= [2.35 \pm 0.08] \times 10^3 \quad \text{for CTEQ3.}
\end{aligned}$$

As we can see in Fig. 4(b), about a half of the total number of events is from initial QG -contributions. Therefore, we can summarize, assuming luminosity $\mathcal{L} = 10pb^{-1}/year$

$$\begin{aligned}
\text{Number of events/year } (p_T \geq 10GeV) &= [1.96 \pm 0.08 \pm 0.16] \times 10^4, \\
\text{Number of events/year } (p_T \geq 40GeV) &= [2.27 \pm 0.08 \pm 0.08] \times 10^3,
\end{aligned}$$

where the first error is due to structure functions, and the second is from scale (Q^2) dependence. For $p_T \geq 10$ GeV (see Fig. 4(a)), the total errors are about 9%, and the QG -contributions are only about 30%. On the other hand, we note that for $p_T \geq 40$ GeV the initial QG -contributions are comparable to the QQ -ones (see Fig. 4(b)), and the theoretical errors are also reduced to 5%. Therefore, for large p_T minimum cut we can investigate gluon structure functions with less theoretical uncertainties. Moreover, we can see from Fig. 4(b) that QG -contributions are even larger than QQ -ones at large rapidity region. It means that $(Q(x_q) + G(x_g))$ -scattering contributions are dominant at large $(x_q - x_g)$, where x_q and x_g are momentum fractions of initial scattering quark and gluon, with the kinematic constraint of $s x_q x_g > M_Z^2$.

Fig. 5 shows rapidity distributions at $\sqrt{s} = 14$ TeV (LHC energies). At these energies, QG -contributions exceed 80% of total cross section. If we consider only $Z + 1jet$ case at these LHC energies, because initial QG -scatterings produce only

quark-jet final states, we can investigate quark fragmentation functions using this large p_T hadroproduction of Z -boson. For $p_T \geq 50$ GeV, total number of events at $\sqrt{s} = 14$ TeV is

$$Number\ of\ events/100pb^{-1} = [3.86 \pm 0.06 \pm 0.11] \times 10^5,$$

where the first (second) errors are due to structure function (QCD-scale) dependence.

This process has been already used for other purposes. In recent papers [14], it is reported that the cross sections for W and Z production in $p\bar{p}$ collisions at $\sqrt{s} = 1.8$ TeV are measured at the Fermilab Tevatron colliders for final states; $W \rightarrow e\nu_e$, $Z \rightarrow e^+e^-$, $W \rightarrow \mu\nu_\mu$, and $Z \rightarrow \mu^+\mu^-$. And it is pointed out that assuming the Standard Model couplings, this result can be used to determine the width and mass of the W boson.

Acknowledgements

We would like to thank Sun Kee Kim for his careful reading of manuscript and for his valuable suggestions in experimental aspects. And we also thank E. Reya, W. K. Tung, A. D. Martin, R. C. Roberts and W. J. Stirling for kindly sending us their newest parton structure functions. The work was supported in part by the Korean Science and Engineering Foundation, Project No. 951-0207-008-2, in part by Non-Directed-Research-Fund, Korea Research Foundation 1993, in part by the CTP, Seoul National University, in part by Yonsei University Faculty Research Grant 1995, and in part by the Basic Science Research Institute Program, Ministry of Education, 1995, Project No. BSRI-95-2425.

References

- [1] P. N. Harriman, A. D. Martin, W. J. Stirling and R. G. Roberts, Phys. Rev. **D42** (1990) 798.
- [2] P. Aurenche, R. Baier, M. Fontannaz, J. F. Owens and M. Werlen, Phys. Rev. **D39** (1989) 3275.
- [3] P. Aurenche, R. Baier and M. Fontannaz, Phys. Rev. **D42** (1990) 1440.
- [4] C. S. Kim, A. D. Martin and W. J. Stirling, Phys. Rev. **D42** (1990) 952;
C. S. Kim, Nucl. Phys. **B353** (1991) 87.
- [5] G. Altarelli, R. K. Ellis, M. Greco and G. Martinelli, Nucl. Phys. **B246** (1984) 12.
- [6] C. Davies and W. Stirling, Nucl. Phys. **B244** (1984) 337;
C. Davies, B. Webber and W. Stirling, Nucl. Phys. **B256** (1985) 413.
- [7] P. B. Arnold and M. H. Reno, Nucl. Phys. **B319** (1989) 37.
- [8] R. K. Ellis, G. Martinelli and R. Petronzio, Nucl. Phys. **B211** (1983) 106.
- [9] A. D. Martin, R. C. Roberts and W. J. Stirling, Phys. Rev. **D50** (1994) 6734.
- [10] M. Glück, E. Reya and A. Vogt, Z. Phys. **C53** (1992) 127.
- [11] CTEQ Collaboration: H. L. Lai, *et. al.*, Phys. Rev. **D51** (1995) 4763.
- [12] E. L. Berger, F. Halzen, C. S. Kim and S. Willenbrock, Phys. Rev. **D40** (1989) 83.
- [13] S. D. Ellis and W. J. Stirling, Phys. Lett. **B256** (1991) 258.
- [14] CDF Collaboration: F. Abe, *et. al.*, **hep-ex/9503007**;
D0 Collaboration: S. Abachi, *et. al.*, **hep-ex/9505013**.

Figure Captions

Fig.1 The p_T distributions of $p\bar{p} \rightarrow Z + X$ at $\sqrt{s} = 1.8$ TeV using $Q^2 = M_Z^2$. QQ and QG represent the initial *quark-quark* (or *-antiquark*) and *quark-gluon* contributions respectively, and *total* represents for the sum of all contributions. The solid line is for MRS(A), the dash-dotted is for CTEQ3, and the dashed is for GRV(HO).

Fig.2 The p_T distributions of $p\bar{p} \rightarrow Z + 1jet$ from (QQ) $q\bar{q} \rightarrow Zg$ and (QG) $qg \rightarrow Zg$ ($\bar{q}g \rightarrow Z\bar{q}$) at $\sqrt{s} = 1.8$ TeV using $Q^2 = M_Z^2$. Also shown are the p_T distributions of $p\bar{p} \rightarrow Z + 1jet$ and $Z + 2jets$.

Fig.3 The p_T distributions of $p\bar{p} \rightarrow Z + X$ for $y = 0$, at $\sqrt{s} = 1.8$ TeV using $Q^2 = M_Z^2$. Also shown are the p_T distributions of $QG \rightarrow Z + 1jet$ and $Z + 2jets$ cases for $y = 0$.

Fig.4 The rapidity distributions of $QQ \rightarrow Z + X$ and $QG \rightarrow Z + X$ (a) for $p_T \geq 10$ GeV, and (b) for $p_T \geq 40$ GeV, at $\sqrt{s} = 1.8$ TeV using $Q^2 = M_Z^2$.

Fig.5 The rapidity distributions of $QQ \rightarrow Z + X$ and $QG \rightarrow Z + X$ for $p_T \geq 50$ GeV at $\sqrt{s} = 14$ TeV using $Q^2 = M_Z^2$.

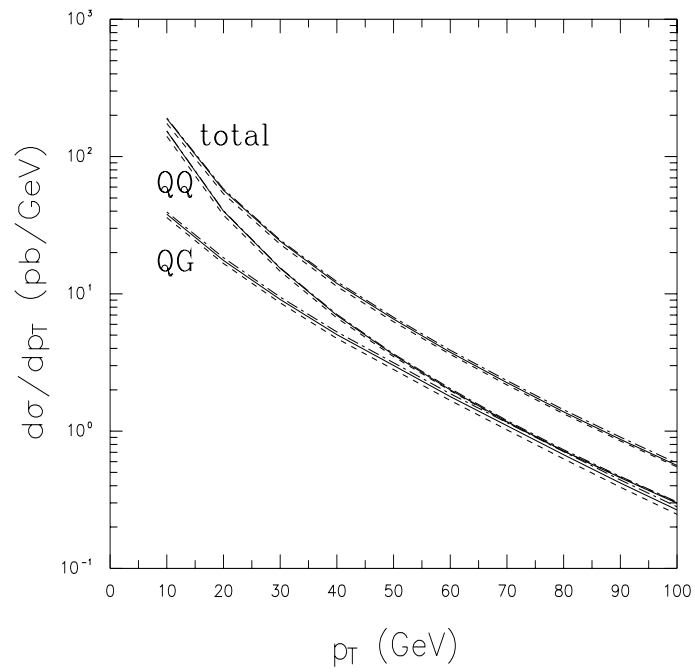


Fig.1

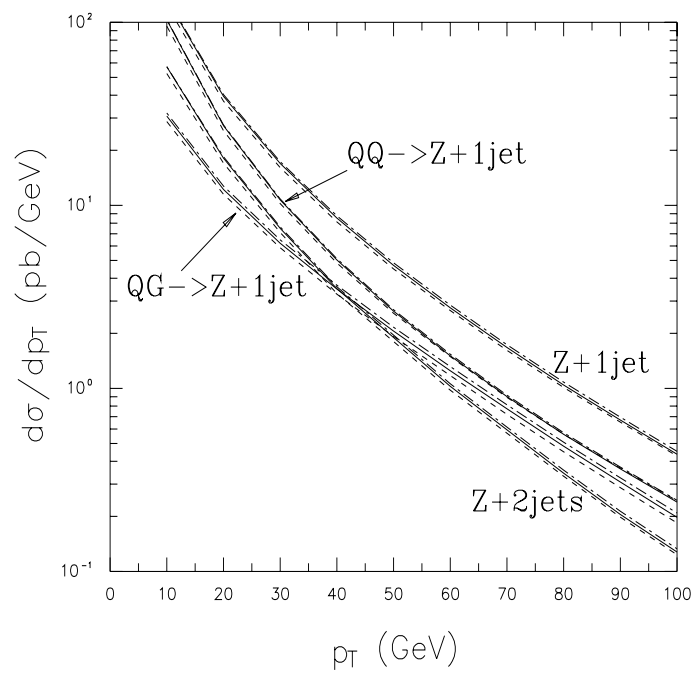


Fig.2

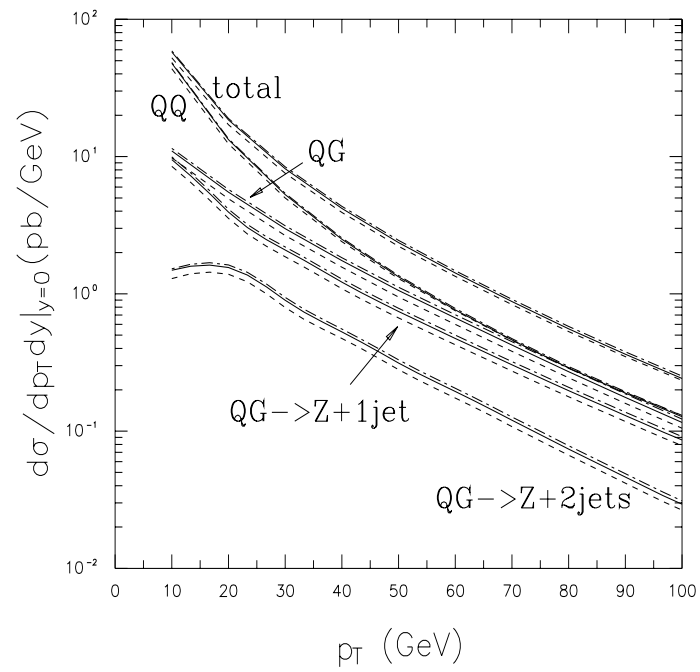


Fig.3

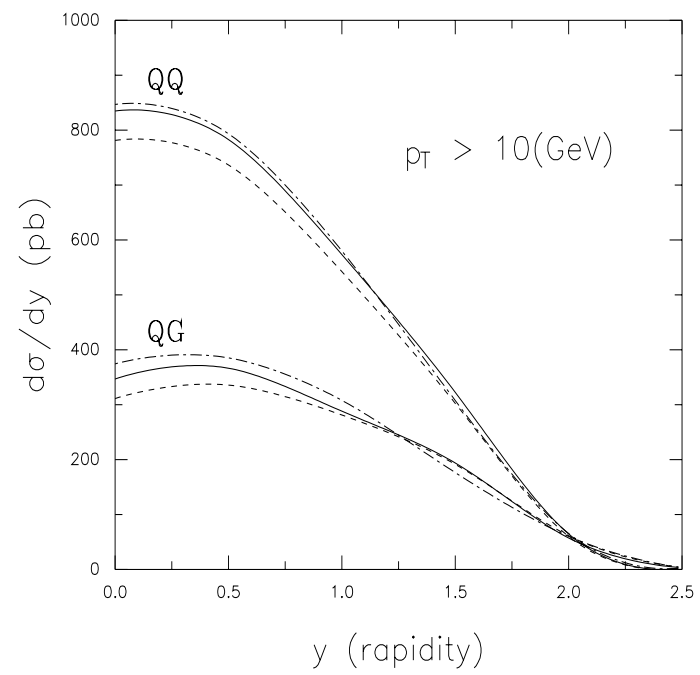


Fig.4(a)

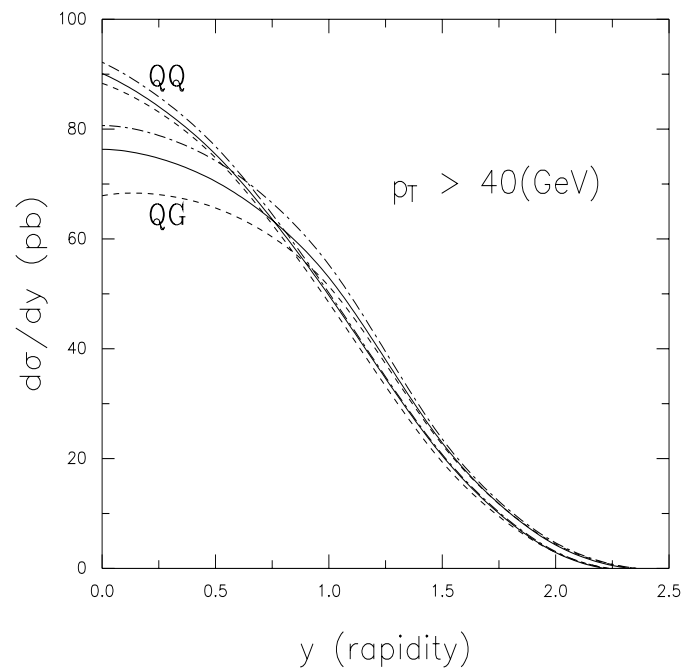


Fig.4(b)

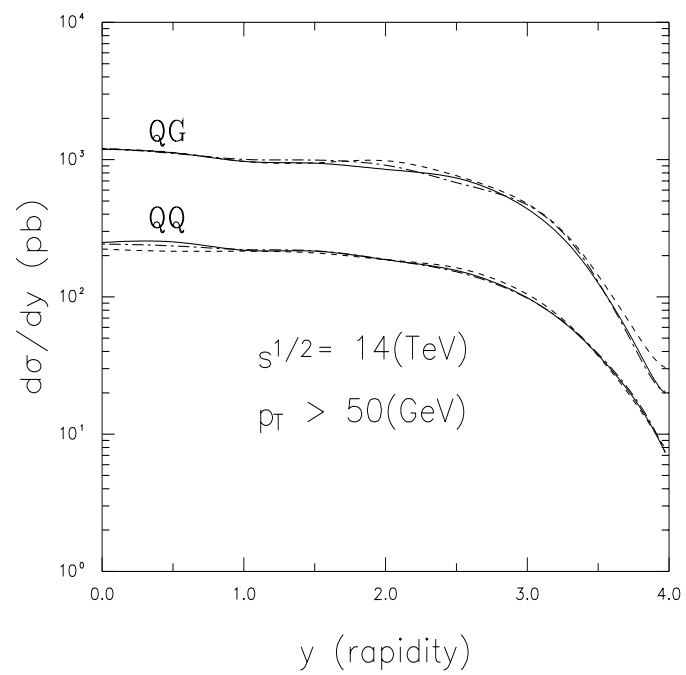


Fig.5